Self-assembled organogels obtained by adding minute concentrations of a bile salt to AOT reverse micelles

Shih-Huang Tung, Yi-En Huang and Srinivasa R. Raghavan*

Received 23rd November 2007, Accepted 27th February 2008
First published as an Advance Article on the web 19th March 2008
DOI: 10.1039/b718145k

The two-tailed anionic surfactant, AOT is well-known to form spherical reverse micelles in organic solvents such as cyclohexane and *n*-alkanes. Here, we report that trace amounts (*e.g.*, around 1 mM) of the dihydroxy bile salt, sodium deoxycholate (SDC) can transform these dilute micellar solutions into self-supporting, transparent organogels. Gels can be obtained at a total AOT + SDC concentration as low as 6 mM or about 2 mg mL^{-1}. Among all the bile salts studied, SDC is the only one that is capable of inducing organogels. The structure and rheology of these organogels is reminiscent of the self-assembled networks formed by proteins such as actin in water. In particular, both classes of gels exhibit the remarkable property of *strain-stiffening*, where the gel stiffness (modulus) increases with strain amplitude. Structurally, both gels are based on entangled networks of long, cylindrical filaments. We propose that SDC forms hydrogen bonds with AOT headgroups, transforming some of the spherical AOT micelles into semiflexible filaments. The average diameter of these filaments has been measured by small-angle neutron scattering (SANS), and suggests that SDC molecules are stacked together in the filament core.

Introduction

Molecular gels are spontaneous assemblies of small molecules into three-dimensional networks that can entrap the solvent *via* surface tension and capillary forces.[1–3] In recent years, the importance of molecular gels in the chemical and biological sciences has become widely recognized. Numerous kinds of gelator molecules have been reported, some that are capable of gelling organic solvents,[1] and others that can gel water.[2] The gelling ability of these molecules is often associated with their ability to form filamentous structures (chains, tubes, tapes, or fibers).[1–3] Individual filaments, in turn, tend to get connected into a network at junction points through physical bonds. A wide range of physical interaction forces have been implicated in gel formation, including hydrogen bonds, metal coordination bonds, electrostatic bonds, van der Waals forces, and hydrophobic interactions.[1–3]

An important motivation for the study of synthetic molecular gels has been their structural resemblance to gels found in nature. Indeed, the gel state characterizes much of biology; in particular, the cytoplasm in eukaryotic cells is a gel formed from filaments of cytoskeletal proteins such as actin and tubulin.[4] Numerous biophysical studies have been conducted on the aqueous assembly of small, globular proteins such as G-actin into filaments (F-actin) and thereby into gel networks.[5–7] Synthetic hydrogel mimics of actin have recently been reported from *de novo*-synthesized peptides.[8,9] However, much of the literature on gels has focused on those formed by organic molecules in non-polar solvents, *i.e.*, "organogels".[1,3] While such organogels are broadly analogous to actin hydrogels, it is generally believed that their structures are fundamentally different. For example, the junctions in many organogels consist of pseudo-crystalline microdomains, which is not the case for actin gels.[1,10] The latter do not need to have specific cross-links or bonds between their filaments; rather, the filaments are so long (~20 μm) that they become tightly entangled and interpenetrated, leading to gel-like behavior.[5,6]

In this paper, we report a new two-component organogel system formed by the synergistic assembly of two amphiphilic molecules. We will highlight some of the unusual features of these gels, including their formation at very low precursor concentrations. More importantly, we will show that these organogels are structurally and rheologically similar to actin hydrogels. In particular, both types of gels are networks of semi-flexible filaments and both show the property of *strain-stiffening*, *i.e.*, an increase in stiffness (gel modulus) with the amplitude of the deformation.[11] This property has been closely associated with biological gels and tissues, and its origin is very much in debate.[11–14] We believe that the biomimetic properties of our organogels may make them an attractive model system for future studies.

The amphiphilic constituents of our organogel are each well-known molecules that have been studied in detail. The major component is the twin-tailed anionic surfactant, sodium bis(2-ethylhexyl) sulfosuccinate (AOT) (Fig. 1). It is widely known that AOT forms spherical reverse micelles in a range of organic solvents and over a range of concentrations.[15] The second component of our organogel system is the bile salt, sodium deoxycholate (SDC) (Fig. 1). Bile salts are physiological surfactants that have been studied extensively in water.[16] In organic solvents, on the other hand, most bile salts, including SDC, are insoluble. Thus, neither AOT nor SDC alone can act as an organogelator.

Department of Chemical & Biomolecular Engineering, University of Maryland, College Park, MD 20742-2111, USA. E-mail: sraghava@eng.umd.edu

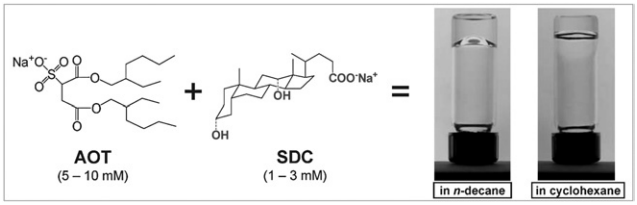

Fig. 1 Molecular structures of the surfactant, AOT and the bile salt, SDC, and photographs of 10 mM AOT + 2 mM SDC organogels in *n*-decane and cyclohexane. The gels are optically clear and support their weight in the inverted vials.

However, when a dilute (*e.g.*, 5–10 mM) reverse micellar solution of AOT in *n*-decane is combined with trace amounts (*e.g.*, 1 mM) of SDC, the result is a transparent organogel that can hold its weight in the inverted vial (Fig. 1). Note that these samples are gels in the strict rheological sense, *i.e.*, in that they have a finite (non-zero) value of the elastic modulus G' at low frequencies.[17]

It is useful to place our investigation in the context of some previous studies with AOT that have dealt with reverse micellization and gelation.[18–22] John and co-workers have shown that certain phenol[18–20] and naphthalene derivatives[21] can also transform AOT reverse micelles into organogels. Thus, AOT organogels can apparently be induced by a variety of molecules, although the gel structure seems to differ from one gelator to the other. For instance, many of the earlier AOT gels were opaque, indicating that they were composed of microscale, hierarchical structures rather than nanoscale filaments.[20] Significantly, our studies with SDC show that it is by far the most efficient gelator for AOT, *i.e.*, it induces AOT organogels at much lower concentrations than the earlier gelators. Further comparison between the AOT–SDC and previous organogel systems is provided in subsequent sections of this paper.

Finally, we should clarify our motivation for studying bile salts, which might seem an unusual choice for a gelator, especially in organic solvents. Our interest in bile salts arose out of our earlier study on mixtures of these molecules with the phospholipid, lecithin in organic solvents – these mixtures formed viscoelastic solutions that were shown to contain reverse wormlike micelles.[23,24] We should reiterate that lecithin–bile salt mixtures were viscoelastic organosols, not gels, *i.e.*, their elastic moduli G' dropped to zero at low frequencies.[23,24] Moreover, a variety of bile salts (not just SDC) could induce lecithin to form viscoelastic organosols.[23] Here, on the other hand, we find that only SDC is capable of inducing AOT to form organogels, and furthermore, AOT–SDC gels are obtained at much lower concentrations compared to viscoelastic lecithin–SDC solutions. Further discussion on the unique nature of SDC as a gel inducer will be provided later in this paper.

Experimental

Materials

The bile salt, SDC (> 97% purity) and the surfactant, AOT (> 98%) were purchased from Sigma–Aldrich. Cyclohexane, deuterated cyclohexane (99.5% D) and *n*-decane were purchased from J. T. Baker, Cambridge Isotopes and Sigma–Aldrich, respectively. All chemicals and solvents were used as received

Sample preparation

Mixed solutions containing AOT and SDC were prepared as follows. First, 100 mM stock solutions of AOT in ethanol and SDC in methanol were prepared. Samples of desired composition were prepared by mixing the stock solutions. The ethanol and methanol were then removed by evaporation in a fume hood for 24 h, and the resulting AOT–SDC film was further dried in a vacuum oven at room temperature for 72 h. The organic solvent (cyclohexane, deuterated cyclohexane or *n*-decane) was then added to this dried film and the sample was stirred till it became transparent and homogeneous. The above procedure ensured the removal of any residual water from the sample and thereby facilitated reproducible sample preparation. Samples were equilibrated for at least 3 days at room temperature prior to conducting experiments.

Rheology

Dynamic rheological experiments were performed on an AR2000 stress-controlled rheometer (TA Instruments) using either parallel-plate or couette geometries, which were both equipped with Peltier-based temperature control. A solvent trap was used to minimize sample evaporation. Frequency spectra were conducted in the linear regime of the samples, as determined from dynamic strain sweep measurements. To prevent the absorption of moisture by the samples during rheological experimentation, it was found to be advantageous to work under conditions when the relative humidity in the laboratory was low (below 20%).

Small-angle neutron scattering (SANS)

SANS measurements were made on the NG-7 (30 m) beamline at NIST in Gaithersburg, MD. Neutrons with a wavelength of 6 Å were selected. Two distances of 1.2 and 15 m between sample and detector were used, so as to yield a range of scattering vector q from 0.004 to 0.4 $Å^{-1}$. Samples for SANS studies were prepared with deuterated cyclohexane and were measured in 1 mm quartz cells at 20 °C. The scattering spectra were corrected and placed on an absolute scale using calibration standards provided by NIST. The data presented here are for the radially averaged intensity I *versus* the scattering vector $q = (4\pi/\lambda)\sin(\theta/2)$, where λ is the wavelength of incident neutrons and θ the scattering angle.

SANS modeling

For dilute solutions of non-interacting scatterers, the SANS intensity $I(q)$ can be modeled purely in terms of the form factor $P(q)$ of the scatterers (*i.e.*, the structure factor $S(q) \rightarrow 1$ in this case). In this study, we considered form-factor models for spherical micelles, rigid cylindrical micelles, and for mixtures of these two shapes. The models were implemented using software modules provided by NIST to be used with the IGOR graphing package. The expressions used in these models are given below. Here, $(\Delta\rho)^2$ is the scattering contrast, $\Delta\rho$ being the difference in scattering length density between the micelle and the solvent.

Spheres

The form factor $P(q)$ for spheres with radius R_s is given by:[25,26]

$$P_{\text{sphere}}(q) = (\Delta\rho)^2\left(\frac{4}{3}\pi {R_s}^3\right)^2\left[\frac{3(\sin(qR_s) - qR_s\cos(qR_s))}{(qR_s)^3}\right]^2 \quad (1)$$

Rigid cylinders

The form factor $P(q)$ for rigid cylinders of radius R_c and length L is given by:[25,26]

$$P_{\text{cylinder}}(q) = (\Delta\rho)^2\left(\pi {R_c}^2 L\right)^2 \int_0^{\pi/2} [F(q,\alpha)]^2 \sin\alpha \; d\alpha \quad (2)$$

where

$$F(q,\alpha) = \frac{J_1(qR_c\sin\alpha)}{(qR_c\sin\alpha)} \cdot \frac{\sin(qL\cos\alpha/2)}{(qL\cos\alpha/2)} \quad (3)$$

Here α is the angle between the cylinder axis and the scattering vector q and $J_1(x)$ is the first-order Bessel function of the first kind.

Coexistence of spheres and rigid cylinders

For coexisting spheres and cylinders, the overall scattering intensity would be the sum of contributions from each type of structure. If the solutions are sufficiently dilute, the overall intensity can be simply expressed by:

$$I_{\text{overall}}(q) = c[\phi_s P_{\text{sphere}}(q) + (1 - \phi_s)P_{\text{cylinder}}(q)] \quad (4)$$

Here c is the overall concentration and ϕ_s is the volume fraction of spheres. The rationale for using this particular model is explained later in the paper.

IFT of SANS data

SANS data were also analyzed by the indirect Fourier transform (IFT) method, which yields particle shape and size without the need for any *a priori* assumptions.[27] To use IFT, first the incoherent background is estimated from the asymptotic slope of a Porod plot (Iq^4 *vs.* q^4) at high q. The scattering intensity $I(q)$ (with incoherent background subtracted) is then Fourier-transformed to obtain the pair distance distribution function $p(r)$ in real space. For non-interacting scatterers, $I(q)$ and $p(r)$ are related by:[27]

$$I(q) = 4\pi \int_0^\infty p(r)\frac{\sin(qr)}{qr}dr \quad (5)$$

$p(r)$ provides information on the shape and size of the scattering entities. In particular, the largest dimension of the scatterers can be estimated, corresponding to the value of r beyond which $p(r) = 0$. IFT analysis was implemented using the commercial PCG software package.

Results

Gel properties: visual observations, birefringence

Photographs of AOT–SDC organogels in cyclohexane and *n*-decane are shown in Fig. 1. Each gel contains 10 mM of AOT and 2 mM of SDC. The gels are shown in inverted vials to indicate that they are rigid enough to support their own weight. Note that the gels are transparent, indicating that their internal structures are in the nanoscale size range. This is in contrast to many organogel systems that tend to be cloudy or opaque – in those cases, the inherent structures are either thick (microscale) fibrils[20] or spherulitic crystallites.[10] The gels do become cloudy as the SDC : AOT molar ratio (X_{SDC}) is increased above 0.25 – however, these samples tend to become unstable with time and are not the focus of our investigation. All gels at low X_{SDC}, however, remain transparent and stable for more than one year when stored in sealed containers.

From a structural standpoint, it is also useful to examine the gels under crossed polarized light. Such a photograph is shown in Fig. 2 for a series of AOT–SDC samples (20 mM AOT, varying SDC). The figure shows that samples above a SDC concentration of 3 mM ($X_{\text{SDC}} = 0.15$) exhibit pronounced birefringence (all these samples are gels). Note that the samples are being examined at rest, *i.e.*, in the absence of any shear. Birefringence at rest in organogels is usually indicative of spherulites;[10] however, no such structures could be observed by optical microscopy. An alternate source of static birefringence can arise from the spontaneous alignment of filamentous structures in solution. In particular, it is known that a dispersion of rods or filaments can undergo a transition from an isotropic to a nematic phase (where the particles show 1-dimensional order) as the size and/or volume fraction of the particles is increased.[28,29] Such a transition is driven by entropy and is referred to as an Onsager transition.[28] Thus the birefringence in Fig. 2 could be indicating that AOT and SDC are self-assembled into rather rigid filaments and that there is a continuous lyotropic phase transition[29] whereby these filaments align to produce nematic gels.

We believe that AOT–SDC gels do indeed contain filaments, and we will corroborate this aspect using SANS later in the paper. However, these gels are unlikely to be true nematics, *i.e.*, there is no thermodynamic transition to an ordered phase in these systems. In this context, the thermal behavior of these gels is revealing. As the birefringent gels are heated to about 80 °C, the gels undergo "melting",[1] *i.e.*, they are transformed from self-supporting solids to thin liquids (see below). This melting transition is thermoreversible, *i.e.*, the gel reforms when the sample is cooled. However, the cooled gels no longer exhibits strong birefringence. If the gel is now shaken vigorously, the birefringence reappears and it does not go away (samples are still strongly birefringent after more than a year). The interpretation here is that the filaments in AOT–SDC gels become aligned

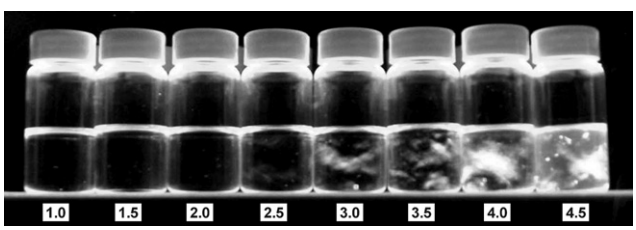

Fig. 2 Photographs under crossed polarizers of AOT–SDC gels in cyclohexane. The AOT concentration is 20 mM and the SDC concentration (in mM) is indicated below each vial. The gels at higher SDC concentrations show strong birefringence.

by shear, but this alignment is locked in by the volume-filling network.[30] Interestingly, gels of F-actin also have similar properties: they show a persistent birefringence at high concentrations that was initially believed to be indicative of a thermodynamic, 1st order phase transition,[7,29] but more recently has been correlated with the shear-alignment of F-actin filaments into domains.[30] The similarities with actin gels will be a recurring theme in this paper.

Gel properties: effects of temperature, humidity

As mentioned above, gels of AOT–SDC melt when heated above a characteristic melting temperature T_m. This melting is abrupt, *i.e.*, the sample remains a self-supporting gel up to T_m, but then it rapidly melts at T_m. Such abrupt melting is characteristic of organogels,[1] whereas viscoelastic organosols show a steady, exponential drop in viscosity with temperature.[24] We have studied the variation of T_m with gel composition – these experiments were done for AOT–SDC gels in *n*-decane. T_m was determined by a combination of visual and rheological methods. We found that T_m occurred at *ca.* 80 °C independent of the SDC : AOT ratio and increased only slightly with AOT concentration (from *ca.* 79 to 83 °C over an AOT concentration range from 25 to 100 mM). Another point to be addressed is the thermoreversibility – as mentioned, melted gels could be re-solidified upon cooling back to room temperature. However, if a gel was heated well beyond T_m (*e.g.*, to about 90 °C), a precipitate formed in the sample and it did not reform upon cooling. This irreversible precipitation could be due to the thermal degradation or hydrolysis of the precursor molecules (AOT or SDC) at these high temperatures.

Another interesting property of AOT–SDC organogels is that they are very sensitive to water, and thereby to humidity. The addition of trace quantities of water is enough to liquefy the gel. Similarly, if a sample vial is left open and thereby exposed to atmospheric humidity for a few hours, the gel will often melt. Such sensitivity to moisture has been noted before by John and co-workers[18,19] for their AOT organogels that were induced by phenolic compounds. This behavior strongly implies that hydrogen bonding is the driving force for self-assembly and gel formation – the action of water in disrupting the gel can then be attributed to the disruption of hydrogen bonds by water molecules.[18,19]

Gel properties: linear rheology

We used dynamic rheological techniques to study the onset and evolution of AOT–SDC gels as a function of composition. Our initial focus will be on the linear sample response at low strain amplitudes and as a function of frequency. Fig. 3 shows trends as a function of SDC content at fixed AOT – data are shown at 20 °C for samples in cyclohexane containing 10 mM AOT. Note that a 10 mM solution of AOT alone in cyclohexane contains spherical reverse micelles and its viscosity is close to that of the solvent. Fig. 3a shows that adding just 0.5 mM of SDC ($X_{SDC} = 0.05$) converts the AOT micellar solution into a viscoelastic fluid. In this case, the elastic modulus G' exceeds the viscous modulus G''at high frequencies, indicating elastic behavior, whereas G'' exceeds G' at low frequencies, indicating viscous behavior. The crossover of G' and G'' occurs at a frequency $\omega = 0.01$ rad s^{-1} and the inverse of this frequency gives a characteristic relaxation time of 100 s for this sample. Note that this kind of dynamic spectrum is typical of transient entangled networks (*e.g.*, of polymer chains or wormlike micelles in solution).[17] Increasing the SDC content to 0.75 mM does not change the nature of the response, but the entire frequency spectrum shifts upward to higher moduli. Also, at low frequencies below the crossover point, the slopes of G' and G'' become closer to each other, which indicates the onset of gel formation.[31] As the SDC concentration is increased to 1 mM ($X_{SDC} = 0.1$), the dynamic rheological response becomes characteristic of an organogel (Fig. 3c). Here G' is nearly independent of frequency and exceeds G'' over the entire range of frequencies, indicating that the gel is an elastic material with an infinite relaxation time (and thereby an infinite viscosity).[17,31] The level of G' characterizes the strength and stiffness of the gel, and can be termed the gel modulus.[17,31]

Next, we describe trends in rheology as a function of the overall (AOT + SDC) concentration. These experiments were done at a constant SDC : AOT ratio, $X_{SDC} = 0.2$. Data at 20 °C for a series of these samples in cyclohexane are shown in Fig. 4. We observe that combining just 2.5 mM AOT with 0.5 mM SDC gives rise to a strongly viscoelastic solution (Fig. 4a). Here, G' and G'' cross at a frequency $\omega = 0.004$ rad s^{-1}, indicating a relaxation time of 250 s for the sample. As the concentration is increased to 5 mM AOT and 1 mM SDC (Fig. 4b), we find the onset of a gel-like response. Note again that G' is frequency-independent and exceeds G'' over the frequency range, *i.e.*, the sample satisfies the strict rheological definition of a gel.[17,31] Increasing the concentration to 7.5 mM AOT and 2.5 mM SDC makes the gel stronger, *i.e.*, the value of G' becomes higher (Fig. 4c). The above rheological data thus show that very low concentrations of AOT and SDC are enough to produce organogels. Fig. 5 shows the scaling of gel modulus G'

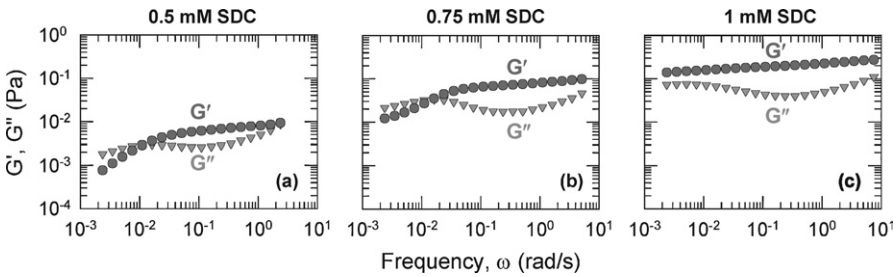

Fig. 3 Dynamic rheology at 20 °C of three AOT–SDC mixtures in cyclohexane, each containing 10 mM AOT and with varying SDC concentrations (indicated on the plots). Each plot shows the elastic modulus G' (circles) and the viscous modulus G'' (triangles) as functions of frequency ω.

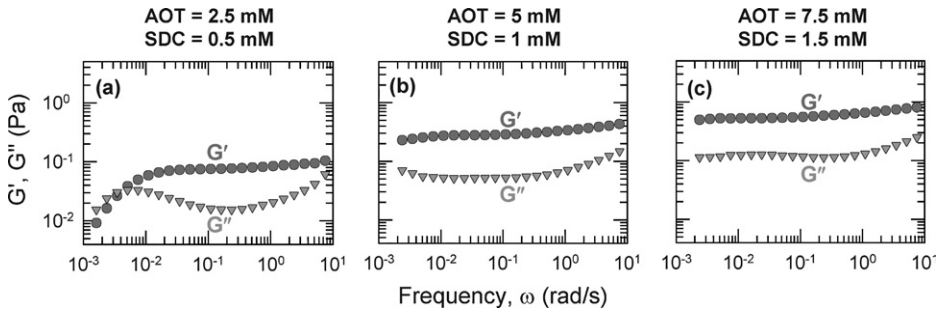

Fig. 4 Dynamic rheology at 20 °C of three AOT–SDC mixtures in cyclohexane with a constant molar ratio of SDC : AOT = 0.2 and with varying overall concentration. The composition of each sample is indicated on the corresponding plot. Each plot shows the elastic modulus G' (circles) and the viscous modulus G'' (triangles) as functions of frequency ω.

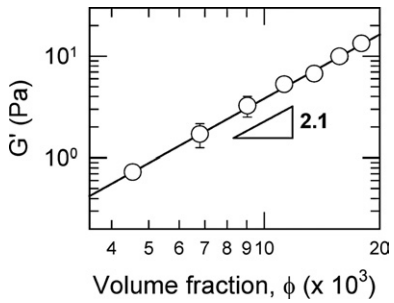

Fig. 5 Elastic modulus at 20 °C of AOT–SDC mixtures in cyclohexane as a function of the total amphiphile volume fraction ϕ. The SDC : AOT molar ratio is 0.15 in all these samples. The solid line through the data corresponds to a scaling of $G' \sim \phi^{2.1}$.

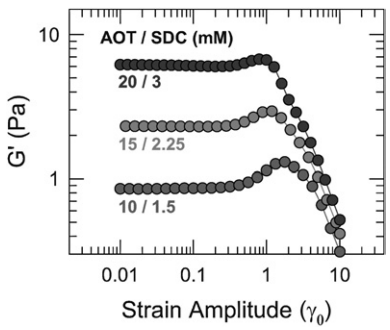

Fig. 6 Strain-stiffening response at 20 °C of AOT–SDC samples in cyclohexane (SDC : AOT molar ratio = 0.15 in all cases). All samples show an increase in their elastic modulus G' over a range of strain amplitudes, *i.e.*, they exhibit strain-stiffening.

with overall volume fraction ϕ of the amphiphiles (AOT + SDC) for a molar ratio $X_{SDC} = 0.15$. G' increases with ϕ according to a power law with an exponent of 2.1. This exponent is close to that found for gels of semiflexible biopolymers such as actin, where the values range from 2.0 to 2.2.[32]

Gel properties: non-linear rheology (strain-stiffening)

We now briefly discuss the non-linear rheology of AOT–SDC organogels, *i.e.*, their response at high deformations exceeding the linear viscoelastic regime. Fig. 6 shows the dependence of elastic modulus G' on strain-amplitude γ at a constant frequency of 10 rad s^{-1}. Data are shown for gels with different (AOT + SDC) concentrations and a constant $X_{SDC} = 0.15$. In the low-strain regime ($\gamma < 0.3$), G' is a constant ($= G_0$), representing the linear response. As the strain-amplitude of the deformation is increased, there is an increase in G' to a maximum value ($= G_{max}$) followed by an abrupt decrease. This increase in G' *vs.* γ is termed strain-stiffening or strain-hardening or strain-thickening by different researchers.[11–14] Note that an increase with strain-amplitude is also seen for G'', but the focus is usually on G' since it is the parameter that most correlates with the network structure. Similar behavior is also seen at other frequencies as well. Fig. 6 also shows that the magnitude of the strain-stiffening effect (*i.e.*, the ratio G_{max}/G_0) is higher at lower amphiphile concentrations. As the AOT–SDC network becomes more dense (*e.g.*, at overall concentrations exceeding 25 mM), strain-stiffening becomes negligible.

To put strain-stiffening in perspective, it is worth noting that most polymeric or colloidal networks generally show strain-thinning, where G' decreases with γ beyond the linear regime.[17] Strain-thinning can be understood to occur due to the deformation-induced rupture of the physical bonds in the network.[17] Strain-stiffening, on the other hand, is unusual because it implies that the network becomes stiffer when it is deformed compared to its stiffness at rest.[11] In effect, the tendency to stiffen makes the network become more resistant to rupture. Interestingly, strain-stiffening has been seen in a range of soft biological materials (*e.g.*, blood clots, cornea, blood vessels) and biopolymer networks, leading some researchers to speculate that the added resistance at large deformations is a material property that has useful biological relevance.[11] A model system for laboratory studies on strain-stiffening has been gels of F-actin.[12,13] Significantly, actin gels show the same trends as a function of concentration as seen in Fig. 6, *i.e.*, the magnitude of strain-stiffening in these gels drops with increasing actin concentration.[12,13]

Gel structure: SANS

Finally, we turn to SANS to elucidate the microstructure of AOT–SDC gels. For these experiments, samples were made in deuterated cyclohexane (these samples were identical to those in cyclohexane). The AOT concentration was fixed at a relatively low value of 20 mM so as to minimize interactions (structure factor effects) between the assemblies. SANS spectra (I *vs.* q) for 20 mM AOT solutions containing varying amounts of

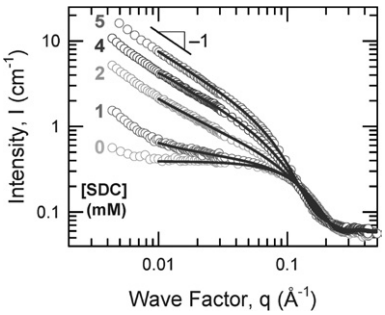

Fig. 7 SANS data from samples in deuterated cyclohexane containing 20 mM AOT and different SDC concentrations. The solid curves through the data are fits to appropriate models (see text for details).

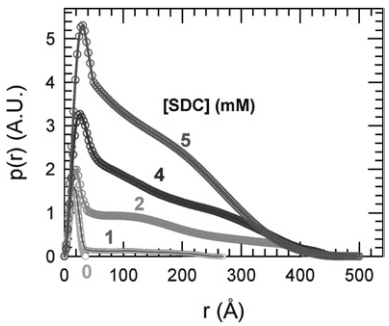

Fig. 8 Pair distance distribution functions $p(r)$ obtained by IFT analysis of the SANS data shown in Fig. 7 for 20 mM AOT + SDC samples in deuterated cyclohexane.

SDC (from 0 to 5 mM) are shown in Fig. 7. It is clear that the addition of SDC causes a dramatic increase in the low-q scattering, while there are slight (but important) changes at higher q as well. The increase in low-q scattering is consistent with a transformation of spherical AOT micelles into elongated structures (note also the asymptotic slope of -1 at low q, which is indicative of cylinders).[26] Thus, SANS confirms the growth of filamentous structures upon addition of SDC to AOT solutions.

Further insight can be obtained by modeling the SANS data using appropriate form factors (eqn (1)–(4)). Model fits are shown as solid lines through the data in Fig. 7, and we focus on the data at $q > 0.01$. First, for the case of AOT alone in cyclohexane, we can adequately model the micelles as spheres (eqn (1)) with radii of 16 Å, in agreement with other studies.[15] As SDC is added, we expect the spheres to grow into cylinders; however, we cannot fit the SANS data for AOT–SDC samples assuming cylinders alone to be present (eqn (2)) (in particular, the fits break down at high q, where SANS mainly probes the cross-section of the micelles). We therefore hypothesize that the AOT–SDC samples contain co-existing populations of spherical micelles and cylindrical filaments. This can be rationalized if we assume that at these low molar ratios of SDC : AOT, the SDC collects in only some of the AOT spherical micelles, which in turn grow while the rest remain intact. Accordingly, we use eqn (4) to model the data, and this yields excellent fits. From the fit parameters (Table 1), we infer that all samples contain co-existing spheres with radii of 16 Å (consistent with pure AOT micelles) and cylinders of radii 22 Å. With increasing SDC, the key parameter that changes is the fraction of cylinders, which increases from 0 (no SDC) to 60% (at SDC = 5 mM). In turn, an increasing fraction of cylindrical filaments correlates with the onset of gel-like behavior in the sample.

Table 1 Parameters from SANS modeling of AOT + SDC samples in d-cyclohexane. The AOT concentration is 20 mM in all samples

[SDC]/mM	R_s/Å[a]	R_c/Å[b]	ϕ_s[c]	ϕ_c[d] $= 1 - \phi_s$
0	16	—	1	0
1	16	22	0.97	0.03
2	16	22	0.81	0.19
4	16	22	0.57	0.43
5	16	22	0.40	0.60

[a] R_s: radius of spheres. [b] R_c: radius of cylinders. [c] ϕ_s: volume fraction of spheres. [d] ϕ_c: volume fraction of cylinders.

The notion of co-existing spherical micelles and cylindrical filaments might appear unusual, although a similar idea has been proposed earlier for other AOT-based organogels.[22] To further substantiate this claim, we have resorted to modeling the SANS data in a different way, using the IFT technique. This method allows SANS data to be analyzed without assuming *a priori* if spheres or cylinders are present.[27] Pair distance distribution functions $p(r)$ from IFT are shown in Fig. 8 for the $I(q)$ data from Fig. 7. For the pure AOT solution, $p(r)$ is symmetrical, and this is typical of spherical micelles.[27] The point where $p(r)$ meets the x-axis gives the micelle diameter, which is 33 Å in this case, in good agreement with the value obtained above. Next, we examine how $p(r)$ changes upon addition of SDC. Note that if only cylinders are present, $p(r)$ should show an inflection point followed by a linear decrease to zero at a value of r equal to the cylinder length.[27,33] However, the $p(r)$ curves for AOT–SDC mixtures are not consistent with either spherical or cylindrical structures alone. For example, the $p(r)$ for 1 mM SDC initially tracks the symmetrical curve of pure AOT, but then it has a further tail that extends up to 270 Å. Likewise, the $p(r)$ curves for 2 and 4 mM SDC have inflection points at 36 and 45Å, respectively, followed by shoulders at higher values of r and eventual drops to zero above 400 Å. These complex $p(r)$ curves imply a co-existence of spheres and cylinders, although it is difficult to deconvolute their individual sizes.[33] Nevertheless, IFT does offer model-independent confirmation for the presence of two distinct types of structures in AOT–SDC samples, in agreement with our direct SANS modeling. Why do only some AOT spherical micelles grow into cylindrical filaments? The answer is discussed in the next section, where we also explain why the value of cylinder radius of 22 Å is significant.

Discussion

We have shown using SANS that the bile salt, SDC transforms spherical AOT micelles into cylindrical filaments. As the SDC : AOT ratio is increased, the number density of these filaments increases and so does their length. When the filaments are sufficiently numerous and long, we believe they form a highly interpenetrated and entangled network, leading to gel-like behavior of the sample.[32] Note that there is no evidence for any other types of physical or chemical cross-links in AOT–SDC networks. Such gel formation simply by entanglement of long, semi-flexible filaments is directly analogous to

that occurring with biopolymers such as actin[5,32] (in the absence of cross-linking proteins). One might argue that the filaments in both AOT–SDC and actin networks will indeed relax by reptation at extremely long times since they are not constrained by cross-links. However, for all practical purposes the samples behave as gels, *i.e.*, as permanent networks,[5,32] and they also satisfy the rheological definition of a gel[17,31] (Fig. 3 and 4).

Structure of AOT–SDC filaments

Given that AOT–SDC samples behave as gels due to the presence of filaments, we still need to explain why SDC induces these filaments to form. Also, why do filaments co-exist with spherical micelles, as suggested by SANS? To answer these questions, we need to know how SDC molecules are distributed within the filaments. Being insoluble in non-polar solvents, SDC can either orient next to the AOT molecules at the interface, or it could arrange in the core of the filament. If the SDC were oriented at the interface, the radius of the filament would be close to that of AOT spherical micelles (*i.e.*, 16 Å). However, from SANS, we estimated a larger filament radius of 22 Å (*i.e.*, diameter of 44 Å). We suggest that this larger radius can be explained only by assuming that the SDC molecules are *stacked in the filament core* and surrounded by AOT molecules. This scenario is depicted in Fig. 9 and it envisions that SDC molecules are arranged with their hydrophilic faces close to the AOT headgroups while their hydrophobic faces are directed towards the center of the filament. Thus, the core of AOT micelles provides a hydrophilic environment in which SDC can stack, with the driving force being the strong hydrogen bonding between AOT headgroups and the hydroxyl groups on the outer face of SDC.

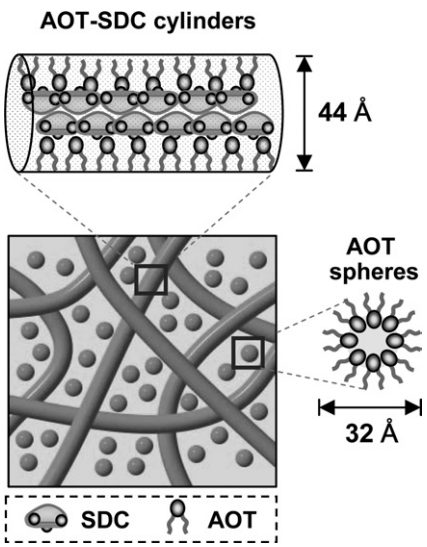

Fig. 9 Schematic of the structures formed when AOT and SDC are added to non-polar liquids (oils). AOT is represented as a molecule with a head and two tails, while SDC is represented as a facial amphiphile. AOT alone tends to form spherical reverse micelles in oil. When small amounts of SDC are added, the SDC preferentially segregates in some of these spheres, causing their transformation into long cylinders. The remaining AOT spheres remain intact and coexist with the cylinders. Based on their radii from SANS, the cylinders are expected to comprise stacks of SDC surrounded by AOT molecules.

The above model for AOT–SDC filaments can be used to explain several aspects. First, we mentioned earlier that among all the bile salts we have studied (the others being sodium cholate, sodium taurocholate, and sodium taurodeoxycholate), SDC is the only one that induces AOT to form organogels. SDC is known to be one of the most hydrophobic bile salts, and significantly, it is the only bile salt that can directly form a hydrogel in water.[34,35] This gel has been shown to consist of helical fibrils formed by the stacking of SDC molecules.[34,35] Thus, SDC has a proven tendency to stack, and the radius of its fibrils was determined to be about 9 Å by X-ray diffraction.[35] Combining the above fibril radius with the length of a fully extended AOT molecule (13 Å), we obtain a net figure of 22 Å, which nicely matches with the filament radius from SANS modeling. This agreement supports the structural model in Fig. 9. It also follows from this model that the binding of SDC to AOT must be a *highly co-operative* process, *i.e.*, for a filament to form, there has to be a sufficient number of SDC molecules in the core. This readily explains why filaments must co-exist with native AOT micelles; in other words, only a few spheres can grow into filaments when only a few SDC molecules are present (*i.e.*, at low SDC : AOT molar ratios). All in all, we believe the unique ability of SDC to stack and form fibrils is a key to its organogel-inducing ability.

Similarities with actin gels

Finally, it is worth summarizing all the features that are shared between AOT–SDC organogels and actin hydrogels. Structurally, both materials are gels simply due to the entanglement of long, semiflexible filaments.[5,32] No other cross-linking agents are necessary to yield a gel, although in the case of actin, the addition of cross-linking proteins can further strengthen the gel.[5,6] Both gels are formed at very low concentrations of precursor molecules (less than 0.2 wt% or 2 mg mL^{-1}).[5–7] In both cases, the initial structures present are spheres (AOT micelles *vs.* G-actin monomers) that transform into filaments upon appropriate conditions. Interestingly, in the case of actin also, a co-existence of filaments and spheres is known to occur during its assembly, quite similar to that shown in Fig. 9.[4,36] Actin filaments are also known to be semiflexible, *i.e.*, their persistence length l_p is comparable to their contour length.[5–7] Although, we have not measured l_p for AOT–SDC filaments, our hypothesis for their structure (with the planar and rigid steroidal rings of SDC in the core, Fig. 9), suggests that these filaments should also be quite rigid.

Actin and AOT–SDC gels have similar properties as well. Both gels show a persistent birefringence, reminiscent of a nematic fluid,[29] although it is more likely to reflect the shear-induced creation of aligned domains that are trapped within the network.[30] Both actin and AOT–SDC gels also exhibit similar rheological response in the linear regime, and their gel moduli scale with concentration in similar ways.[32] Lastly, both types of gels exhibit strain-stiffening, *i.e.*, their gel moduli increase with strain amplitude.[11–13] Even the variation in the magnitude of strain-stiffening with concentration (Fig. 6) are similar for the two classes of gels.[12,13] Currently, the origin of strain-stiffening is a matter of debate and at least two mechanisms have been put forward.[11,14] Both mechanisms, however,

correlate strain-stiffening with the intrinsic rigidity of network filaments. If this is correct, it reiterates that AOT–SDC filaments must be quite rigid, much like actin filaments. Indeed, the rigidity imparted by steroidal bile salt molecules to AOT filaments is analogous to the rigidification of lipid bilayers by addition of steroidal cholesterol.[4]

Conclusions

We have shown that the addition of the bile salt, sodium deoxycholate (SDC) to AOT reverse micellar solutions induces a transition from low-viscosity liquids to elastic and rigid organogels. Organogel formation can be induced by very small (millimolar) amounts of SDC. SANS measurements show that the addition of SDC progressively transforms spherical AOT micelles into long, semiflexible filaments. The gel is believed to form by the entanglement and interpenetration of these filaments within a volume-filling network. Based on SANS data, we suggest that the filaments consist of an AOT shell surrounding a core of planar and rigid SDC molecules, with the AOT and SDC connected by hydrogen bonds. AOT–SDC gels share many properties with gels of biopolymers such as actin, including their birefringence, gel-like linear rheology, and strain-stiffening in non-linear rheology.

Acknowledgements

We would like to acknowledge NIST for facilitating the SANS experiments. Valuable discussions with Dr Steve Kline (NIST) on SANS modeling and with Dr Lionel Porcar (NIST) on strain-stiffening are also acknowledged. This work was partially funded by a grant from Du Pont.

References

1 P. Terech and R. G. Weiss, *Chem. Rev.*, 1997, **97**, 3133–3159.
2 L. A. Estroff and A. D. Hamilton, *Chem. Rev.*, 2004, **104**, 1201–1217.
3 N. M. Sangeetha and U. Maitra, *Chem. Soc. Rev.*, 2005, **34**, 821–836.
4 B. Alberts. *Molecular Biology of the Cell*, Garland Publishers, New York, 2002.
5 P. A. Janmey, S. Hvidt, J. Peetermans, J. Lamb, J. D. Ferry and T. P. Stossel, *Biochemistry*, 1988, **27**, 8218–8227.
6 P. A. Janmey, S. Hvidt, J. Kas, D. Lerche, A. Maggs, E. Sackmann, M. Schliwa and T. P. Stossel, *J. Biol. Chem.*, 1994, **269**, 32503–32513.
7 J. Kas, H. Strey, J. X. Tang, D. Finger, R. Ezzell, E. Sackmann and P. A. Janmey, *Biophys. J.*, 1996, **70**, 609–625.
8 F. M. Menger and K. L. Caran, *J. Am. Chem. Soc.*, 2000, **122**, 11679–11691.
9 A. P. Nowak, V. Breedveld, L. Pakstis, B. Ozbas, D. J. Pine, D. Pochan and T. J. Deming, *Nature*, 2002, **417**, 424–428.
10 X. Huang, P. Terech, S. R. Raghavan and R. G. Weiss, *J. Am. Chem. Soc.*, 2005, **127**, 4336–4344.
11 C. Storm, J. J. Pastore, F. C. MacKintosh, T. C. Lubensky and P. A. Janmey, *Nature*, 2005, **435**, 191–194.
12 J. Y. Xu, Y. Tseng and D. Wirtz, *J. Biol. Chem.*, 2000, **275**, 35886–35892.
13 M. L. Gardel, J. H. Shin, F. C. MacKintosh, L. Mahadevan, P. Matsudaira and D. A. Weitz, *Science*, 2004, **304**, 1301–1305.
14 P. R. Onck, T. Koeman, T. van Dillen and E. van der Giessen, *Phys. Rev. Lett.*, 2005, **95**.
15 M. Kotlarchyk, J. S. Huang and S. H. Chen, *J. Phys. Chem.*, 1985, **89**, 4382–4386.
16 D. M. Small, *The Bile Acids*, Plenum Press, New York, 1971, vol. 1.
17 C. W. Macosko, *Rheology: Principles, Measurements and Applications*, VCH Publishers, New York, 1994.
18 X. D. Xu, M. Ayyagari, M. Tata, V. T. John and G. L. McPherson, *J. Phys. Chem.*, 1993, **97**, 11350–11353.
19 M. Tata, V. T. John, Y. Y. Waguespack and G. L. McPherson, *J. Am. Chem. Soc.*, 1994, **116**, 9464–9470.
20 B. A. Simmons, C. E. Taylor, F. A. Landis, V. T. John, G. L. McPherson, D. K. Schwartz and R. Moore, *J. Am. Chem. Soc.*, 2001, **123**, 2414–2421.
21 Y. Y. Waguespack, S. Banerjee, P. Ramannair, G. C. Irvin, V. T. John and G. L. McPherson, *Langmuir*, 2000, **16**, 3036–3041.
22 P. J. Atkinson, M. J. Grimson, R. K. Heenan, A. M. Howe and B. H. Robinson, *J. Chem. Soc., Chem. Commun.*, 1989, 1807–1809.
23 S. H. Tung, Y. E. Huang and S. R. Raghavan, *J. Am. Chem. Soc.*, 2006, **128**, 5751–5756.
24 S. H. Tung, Y. E. Huang and S. R. Raghavan, *Langmuir*, 2007, **23**, 372–376.
25 L. A. Feigin; D. I. Svergun, *Structure Analysis by Small-Angle X-Ray and Neutron Scattering*, Plenum Press, New York, 1987.
26 J. S. Pedersen, *Adv. Colloid Interface Sci.*, 1997, **70**, 171–210.
27 O. Glatter, *J. Appl. Crystallogr.*, 1977, **10**, 415–421.
28 L. Onsager, *Ann. N. Y. Acad. Sci.*, 1949, **51**, 627–659.
29 J. Viamontes and J. X. Tang, *Phys. Rev. E: Stat. Phys., Plasmas, Fluids, Relat. Interdiscip. Top.*, 2003, **67**.
30 E. Helfer, P. Panine, M. F. Carlier and P. Davidson, *Biophys. J.*, 2005, **89**, 543–553.
31 H. H. Winter and F. Chambon, *J. Rheol.*, 1986, **30**, 367–382.
32 F. C. Mackintosh, J. Kas and P. A. Janmey, *Phys. Rev. Lett.*, 1995, **75**, 4425–4428.
33 T. S. Davies, A. M. Ketner and S. R. Raghavan, *J. Am. Chem. Soc.*, 2006, **128**, 6669–6675.
34 D. M. Blow and A. Rich, *J. Am. Chem. Soc.*, 1960, **82**, 3566–3571.
35 A. A. D'Archivio, L. Galantini, E. Giglio and A. Jover, *Langmuir*, 1998, **14**, 4776–4781.
36 A. I. Norman, R. Ivkov, J. G. Forbes and S. C. Greer, *J. Chem. Phys.*, 2005, **123**.